



Anomalous Meissner effect in pnictide superconductors

R. Prozorov,^{1,*} M. A. Tanatar,¹ Bing Shen,² Peng Cheng,² Hai-Hu Wen,² S. L. Bud'ko,¹ and P. C. Canfield¹

¹The Ames Laboratory and Department of Physics & Astronomy, Iowa State University, Ames, Iowa 50011, USA

²Institute of Physics, Chinese Academy of Sciences, Beijing 100190, China

(Received 22 October 2010; revised manuscript received 5 November 2010; published 18 November 2010)

The Meissner effect has been studied in $\text{Ba}(\text{Fe}_{0.926}\text{Co}_{0.074})_2\text{As}_2$ and $\text{Ba}_{0.6}\text{K}_{0.4}\text{Fe}_2\text{As}_2$ single crystals and compared to well known, type-II superconductors $\text{LuNi}_2\text{B}_2\text{C}$ and V_3Si . Whereas flux penetration is mostly determined by the bulk pinning (and, perhaps, surface barrier) resulting in a large negative magnetization, the flux expulsion upon cooling in a magnetic field is very small, which could also be due to pinning and/or surface-barrier effects. However, in stark contrast with the expected behavior, the amount of the expelled flux increases almost linearly with the applied magnetic field, at least up to our maximum field of 5.5 T, which far exceeds the upper limit for the surface barrier. One interpretation of the observed behavior is that there is a field-driven suppression of magnetic pair breaking.

DOI: [10.1103/PhysRevB.82.180513](https://doi.org/10.1103/PhysRevB.82.180513)

PACS number(s): 74.25.Ha, 74.25.Op, 74.70.Xa, 74.70.Ad

In textbooks,^{1,2} the Meissner effect³ is considered to be the definitive mark of bulk superconductivity. In practice, however, there are various factors that determine the behavior of a real, finite specimen in a magnetic field.^{1,4–6} Nevertheless, in all cases reported so far, the following characteristic behavior has been observed: magnetization measured as a function of an applied magnetic field after cooling the sample in *zero* field is negative and linear in field up to a characteristic penetration field, H_p . Above this field, Abrikosov vortices penetrate the sample and magnetization amplitude decreases.⁵ The value of H_p depends on various parameters, such as sample shape, surface quality, anisotropy, and even pairing symmetry, and ranges between the first critical field, H_{c1} , and the thermodynamic critical field, H_c . For example, in the simplest case without demagnetization when a magnetic field is parallel to the sample surface with characteristic roughness σ , the Bean-Livingston barrier^{1,5,7} field is given by⁸

$$H_p = \frac{\phi_0}{4\pi\lambda\sigma} \ln \frac{e\sigma}{\xi}, \quad (1)$$

which ranges between $H_{c1} \leq H_p \leq H_c$ for $\lambda \leq \sigma \leq \xi$. In the field-cooled (FC) experiment, the resulting magnetic moment at low temperatures depends on the competition between Meissner expulsion, temperature-dependent pinning strength and surface-barrier effects. [Note that we use “FC” to indicate the process when the measurements are taken upon cooling, sometimes denoted as FCC. This may somewhat differ from cooling in an applied magnetic field and measuring upon warming, FCW (Ref. 9)]. In all cases, however, this resulting moment would first become increasingly negative in fields comparable to the characteristic field discussed earlier and then will start to increase reaching zero at the upper critical field, H_{c2} . It has been shown that the surface barrier may play an important role in determining the irreversibility in unconventional superconductors close to T_c (Refs. 10 and 11) and may itself be enhanced due to Andreev bound states.^{12,13} When the applied magnetic field is decreased from a large value, $H \gg H_p$ or the sample is cooled at any field, the barrier actually compensates for the Meissner expulsion.^{5,11}

In real samples with pinning, the competition of temperature-dependent critical current, surface barrier, and H_{c1} determines the value of the field-cooled magnetization, M_{FC} , that peaks approximately at H_p and its value is greatly reduced compared to the theoretical Meissner expulsion, $4\pi M_{\text{FC,ideal}} = -HV$, where V is the sample volume. Sadly, this renders standard, field-cooled Meissner effect measurements of little value for the estimation of the “superconducting fraction.” On the other hand, studies of the field-cooled magnetization of exotic superconductors can reveal distinct phenomena when compared to the conventional materials.

Here we report an unusual Meissner effect in which the negative field-cooled magnetization continues to become increasingly negative with increasing applied field up to our maximum fields (of 5.5 T), way past the estimated first or thermodynamic critical fields. One possible interpretation of these data, suppression of the magnetic pair-breaking, is discussed, but completely different mechanisms related to the peculiarities of iron-based superconductors might be involved.

The experiments were performed on single crystals of electron- and hole-doped BaFe_2As_2 . Optimally doped single crystals of $\text{Ba}(\text{Fe}_{0.926}\text{Co}_{0.074})_2\text{As}_2$ (FeCo-122) (Ref. 14) and $\text{Ba}_{0.6}\text{K}_{0.4}\text{Fe}_2\text{As}_2$ (BaK-122) (Ref. 15) were grown out of FeAs flux using high-temperature solution growth techniques. Sample homogeneity was checked by magneto-optical visualization.^{16,17} For comparison, high-quality low-pinning single crystals of known nonmagnetic type-II superconductors, V_3Si (Ref. 18) and $\text{LuNi}_2\text{B}_2\text{C}$,¹⁹ were measured on the same Quantum Design MPMS unit following the same protocols. All samples were slab shaped with dimensions on the order of 2 mm in the ab plane and 0.1–0.3 mm thickness. Several samples of each kind and of different geometries were measured and here we report results obtained on representative crystals. In this work we focus on the case when the magnetic field was oriented along the ab plane to minimize demagnetization effects, but similar results were obtained for the magnetic field along the short dimension, which is along the crystallographic c axis. Also, similar results were obtained by using a vibrating sample magnetometer in applied magnetic fields up to 9 T. To facili-

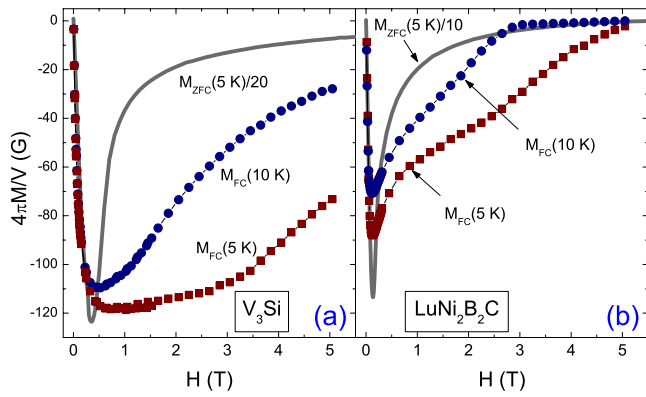


FIG. 1. (Color online) Magnetic moment measured after field cooling, M_{FC} (symbols), and zero field cooling, M_{ZFC} (solid lines) protocols in single crystals of (a) V_3Si and (b) $LuNi_2B_2C$. For $M_{FC}(H)$, each data point was obtained in a separate FC experiment in a constant magnetic field. ZFC curves were scaled by a factor of 20 and 10, respectively.

tate the comparison, magnetization is presented in gauss by calculating $4\pi M/V$, where M (emu) is the measured magnetic moment and V (cm^3) is the sample volume.

Figure 1 shows the data for two well-studied, conventional (as far as vortex behavior is concerned) type-II superconductors with T_c of the same order as the pnictide systems studied here. In both panels the symbols show a magnetic moment, M_{FC} , measured after cooling in a constant magnetic field to a fixed temperatures of 10 and 5 K. Each data point is the result of a *separate* field-cooling procedure. For comparison, standard magnetization curves obtained after cooling in zero field to 5 K are shown by solid lines. Note the scaling by a factor of 20 and 10 in panels (a) and (b), respectively. As discussed above, such behavior is expected for a regular type-II superconductor. Namely, above H_p , both zero FC (ZFC) and FC magnetic moments decrease in magnitude indicating an increasing density of vortices. Note that despite considerable differences in M_{ZFC} and upper critical fields,^{20,21} the maximum amplitude of the negative field-cooled magnetization of these two systems is quite similar, but even they have far from the ideal value of the Meissner expulsion.

Figure 2 shows similar data obtained on a FeCo-122 crystal. Measurements of M_{FC} , shown at 5 and 15 K, reveal a striking difference in comparison with Fig. 1. The magnetic moment increases in amplitude becoming more negative almost linearly in field all the way up to our largest applied field of 5.5 T. The $M_{ZFC}(H)$ curve, on the other hand, exhibits its standard behavior, similar to the curves shown in Fig. 1.

To further illustrate this unusual effect, Fig. 3(a) shows several $M_{FC}(T)$ curves measured at different applied fields in a FeCo-122 single crystal. The magnetic moment is clearly much more negative at higher fields, except for in the vicinity of T_c , as expected. To examine whether this effect is related to the normal-state response, Fig. 3(b) shows measurements of M_{FC} at 5 and 24 K, i.e., just above T_c . An unscaled M_{ZFC} curve at 5 K is also shown to illustrate the relative magnitudes. As expected and known for the Fe-based superconductors, $M(H)$ above T_c is weakly paramag-

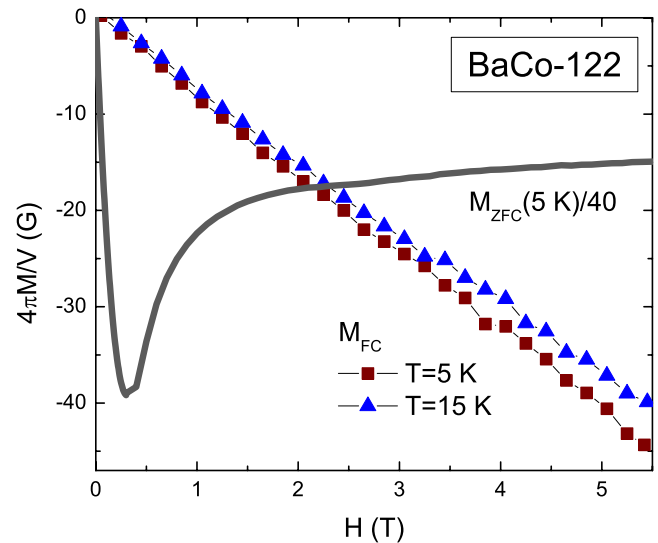


FIG. 2. (Color online) Comparison of M_{FC} (symbols) (sampled at 5 and 15 K) and $M_{ZFC}/40$ (line) measured by sweeping a magnetic field at 5 K in a FeCo-122 crystal.

netic and, therefore, the observed diamagnetism must come from the superconducting state itself.

Similar behavior is observed for BaK-122 crystals. Figure 4(a) shows results of field-cooling experiments as a function of temperature where each curve was obtained by measuring in a constant field indicated in the figure. Figure 4(b) shows the magnetic field dependence of M_{FC} at 5 K along with the $M(H)$ curve measured at 40 K, which is just above T_c as well as unscaled M_{ZFC} at 5 K, for comparison. The inset shows similar data for 20 K indicating that the relative strength of the effect, i.e., magnitudes of M_{FC} vs M_{ZFC} , become even more pronounced. Note that above T_c , M_{ZFC} and M_{FC} experiments produce the same reversible curve for all samples. Overall, the observed behavior is very similar to that of FeCo-122 and is at odds with that of conventional type-II superconductors shown in Fig. 1.

To look at the data from a different angle, Fig. 5 shows the magnetic susceptibility $4\pi\chi = 4\pi M/(VH)$, which should

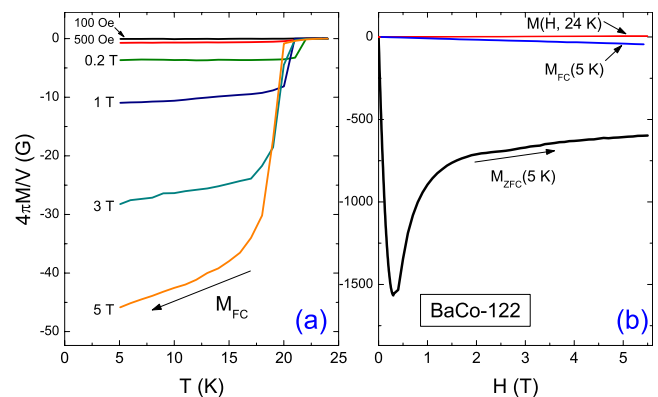


FIG. 3. (Color online) (a) Magnetization measured upon field cooling at different values of the applied magnetic fields in a FeCo-122 crystal. (b) measured M_{ZFC} and M_{FC} at 5 K compared to the magnetization above T_c , where $M_{FC} = M_{ZFC}$.

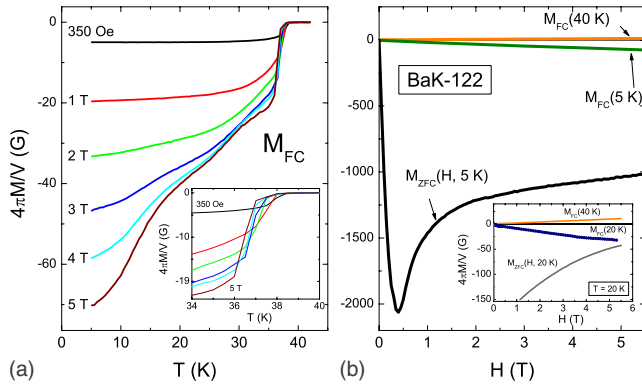


FIG. 4. (Color online) (a) Field-cooled magnetization vs temperature measured at different magnetic fields in a BaK-122 crystal. (b) Measured M_{ZFC} and M_{FC} at 5 K compared to the magnetization above T_c . Inset: similar data for $T=20$ K.

be equal to -1 in the case of an ideal demagnetization-free superconductor and rapidly decrease in amplitude above the characteristic field H_p . Clearly, the field-cooled magnetic susceptibility (shown for 5 and 20 K) is very small, on the order of 1×10^{-3} . It is almost field independent and negative up to our maximum field. Measurements above T_c (at 40 K) reveal field independent, but positive valued susceptibility, as is expected for a paramagnetic response.

The data show a clear difference between conventional type-II superconductors and pnictides. Whereas the values of T_c are comparable in all studied samples, the upper critical fields, H_{c2} , are quite different. In particular, for $H \perp c$ axis, $H_{c2} \sim 55$ T in FeCo-122,^{14,22} 80 T in BaK-122 (Ref. 23) as opposite to 20 T in V_3Si (Ref. 21) and 9 T in $LuNi_2B_2C$.²⁰ Still, the effect is observed in fields much greater than H_{c1} but much lower than H_{c2} , indicating that this is a property of a robust superconducting state with a fully developed order parameter. The negative magnetization upon field cooling is

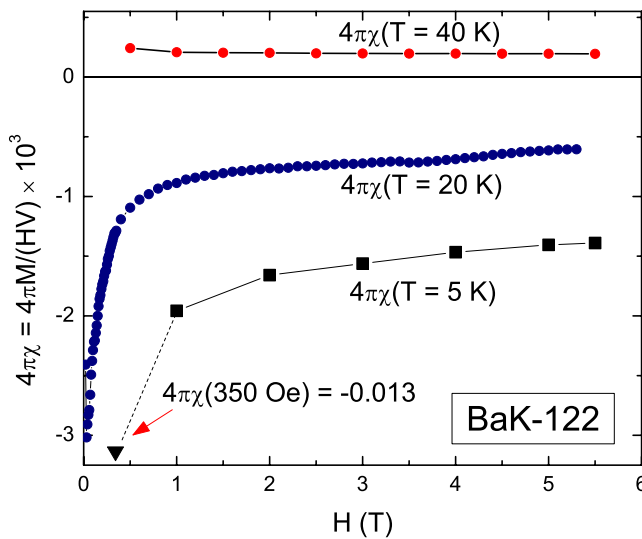


FIG. 5. (Color online) Magnetic susceptibility, $4\pi\chi = M/(VH)$, above (40 K) and below (5 and 20 K) T_c in a BaK-122 crystal. The point at $T=5$ K and $H=350$ Oe, shown by a triangle, is outside the vertical range with $4\pi\chi = -0.013$, still much lower than ideal -1 .

determined by the Meissner effect which has a magnitude that is proportional to the lower critical field, H_{c1} , which is small in pnictides, $H_{c1} \sim 100$ Oe.²⁴ If the observed effect is due to the surface barrier, then following Eq. (1), the maximum critical field (for ideally smooth surface, $\sigma \leq \xi$) where it is effective is of the order of the thermodynamic critical field $H_c \approx \sqrt{H_{c1}H_{c2}} \sim 1$ T if we take the overestimated $H_{c2} \sim 100$ T. In real samples, the surface-barrier field would be less effective due to finite roughness and scattering. Therefore, the conventional Bean-Livingston mechanism does not explain our results.

Another scenario is the competition between bulk pinning and the Meissner effect. Upon cooling, the temperature-dependent pinning prevents some vortices from exiting and a characteristic domelike shape of the magnetic induction is formed with the Meissner expulsion region confined to the sample edges.²⁵ Strong suppression of pinning by a magnetic field could lead to an increase in measured negative magnetization. However, such effect must be clearly visible on the direct measurements of the hysteresis loops with reversible Meissner part dominating the irreversible Bean part. This is not observed in the pnictides.¹⁷ Also, if reversible part of magnetization does not exhibit unusual increase with the increased field, its rapid decrease with field will result in behavior similar to “conventional” Fig. 1.

One interesting possibility is that the magnetic field aligns local magnetic moments of iron ions as well as of vacancies and other lattice disturbances introduced by the doping. These moments act as efficient pair breakers and, therefore, such Zeeman alignment will decrease the pair breaking that involves flipping the spin of the scattering center. Experiments and theory have suggested that such pair-breaking scattering is very important in iron-based superconductors^{26,27} and perhaps our results provide further support for this idea. On the other hand, many theoretical and experimental reports indicate importance of magnetic fluctuations in the mechanism of superconductivity in iron-based superconductors. Therefore, it seems that the pairing and the pair breaking both originate from the same magnetic subsystem and, therefore strength of superconductivity (e.g., transition temperature) should be calculated considering both effects.

The reversible magnetization of a type-II superconductor for $H_{c1} \ll H \ll H_{c2}$ is given by

$$-4\pi \frac{M}{V} = \frac{\phi_0}{8\pi\lambda^2} \ln \frac{\eta H_{c2}}{H}, \quad (2)$$

where $\eta \sim 1$.²⁸ In the strong pair-breaking regime, $\lambda^{-2} \sim \tau_m^2$, where τ_m is the pair-breaking magnetic scattering time. Taking into account the weak paramagnetic response and a relatively small magnetic moment per iron, $m \sim 0.87 \mu_B$ ²⁹ in $BaFe_2As_2$, we can assume a simple correction of the scattering time, $\tau_m = \tau_m(H=0) \exp(mH/k_B T)$. With $m/k_B \leq 0.58$ K/T we can therefore write even at our highest fields and lowest temperatures, $\lambda^{-2} \approx \lambda^{-2}(H=0)(1 + 2mH/k_B T)$.²⁷ Therefore, we would expect that the reversible magnetic moment will increase in amplitude as, $-M \sim H/T$. Surprisingly

enough, this simple model describes our observations quite well. An almost linear field dependence is evident from the Figs. 2–4 and a pronounced temperature dependence is observed, especially at higher fields, see Figs. 3(a) and 4(a). We note that very high upper critical fields of pnictide superconductors are essential for this mechanism to work. Otherwise, the superconducting order parameter gets suppressed and reversible magnetization decreases rapidly, see Eq. (2).

In conclusion, we report on the anomalous field-cooled magnetization in BaFe₂As₂-based superconductors. The magnetic moment becomes progressively more negative as a function of an applied magnetic field that significantly exceeds the thermodynamic critical field. It is proposed that the observed behavior can be explained by a field-induced reduction in magnetic pair breaking. In addition to the pres-

ence of natural magnetic scatterers in iron pnictides, large values of H_{c2} make it possible to observe the effect.

We thank V. G. Kogan, J. R. Clem, A. Gurevich, L. Burlachkov, and E. Phideaux for useful discussions and D. K. Christen for providing V₃Si crystal. The work at The Ames National Laboratory was supported by the U.S. Department of Energy, Office of Basic Energy Sciences, Division of Materials Sciences and Engineering under Contract No. DE-AC02-07CH11358. The work in Beijing (growth of K-doped BaFe₂As₂ crystals and VSM measurement) was partially supported by the Natural Science Foundation of China, the Ministry of Science and Technology of China (973 Project No. 2011CB605900). R.P. acknowledges support from the Alfred P. Sloan Foundation.

*Corresponding author; prozorov@ameslab.gov

- ¹P. G. de Gennes, *Superconductivity of Metals and Alloys* (Benjamin, New York, 1966).
- ²M. Tinkham, *Introduction to Superconductivity* (Dover, New York 1996).
- ³W. Meissner and R. Ochsenfeld, *Naturwiss.* **21**, 787 (1933).
- ⁴A. M. Campbell and J. E. Evetts, *Critical Currents in Superconductors* (Taylor & Francis, London, 1972).
- ⁵J. R. Clem, in *Proceedings of 13th International Conference on Low-Temperature Physics*, edited by K. D. Timmerhaus, W. J. O'Sullivan, and E. F. Hammel (Plenum, New York, 1974), Vol. 3, pp. 102–106.
- ⁶E. H. Brandt, *Rep. Prog. Phys.* **58**, 1465 (1995).
- ⁷C. P. Bean and J. D. Livingston, *Phys. Rev. Lett.* **12**, 14 (1964).
- ⁸Y. A. Genenko, H. Rauh, and S. V. Yampolskii, *J. Phys.: Condens. Matter* **17**, L93 (2005).
- ⁹J. R. Clem and Z. Hao, *Phys. Rev. B* **48**, 13774 (1993).
- ¹⁰M. Konczykowski, L. I. Burlachkov, Y. Yeshurun, and F. Holtzberg, *Phys. Rev. B* **43**, 13707 (1991).
- ¹¹L. Burlachkov, *Phys. Rev. B* **47**, 8056 (1993).
- ¹²C. Iniotakis, T. Dahm, and N. Schopohl, *Phys. Rev. Lett.* **100**, 037002 (2008).
- ¹³G. Leibovitch, R. Beck, A. Kohen, and G. Deutscher, [arXiv:0901.1774](https://arxiv.org/abs/0901.1774) (unpublished).
- ¹⁴N. Ni, M. E. Tillman, J.-Q. Yan, A. Kracher, S. T. Hannahs, S. L. Bud'ko, and P. C. Canfield, *Phys. Rev. B* **78**, 214515 (2008).
- ¹⁵H. Luo, Z. Wang, H. Yang, P. Cheng, X. Zhu, and H.-H. Wen, *Supercond. Sci. Technol.* **21**, 125014 (2008).
- ¹⁶R. Prozorov, N. Ni, M. A. Tanatar, V. G. Kogan, R. T. Gordon, C. Martin, E. C. Blomberg, P. Prommapan, J. Q. Yan, S. L. Bud'ko, and P. C. Canfield, *Phys. Rev. B* **78**, 224506 (2008).

- ¹⁷R. Prozorov, M. A. Tanatar, E. C. Blomberg, P. Prommapan, R. T. Gordon, N. Ni, S. L. Bud'ko, and P. C. Canfield, *Physica C* **469**, 667 (2009).
- ¹⁸G. V. Samsonov and V. S. Neshpor, *Zh. Eksp. Teor. Fiz.* **3**, 1143 (1956) [*Sov. Phys. JETP* **3**, 947 (1957)].
- ¹⁹P. C. Canfield, P. L. Gammel, and D. J. Bishop, *Phys. Today* **51**(10), 40 (1998).
- ²⁰V. Metlushko, U. Welp, A. Koshelev, I. Aranson, G. W. Crabtree, and P. C. Canfield, *Phys. Rev. Lett.* **79**, 1738 (1997).
- ²¹M. Khlopkin, *JETP Lett.* **69**, 26 (1999).
- ²²M. Kano, Y. Kohama, D. Graf, F. Balakirev, A. S. Sefat, M. A. Mcguire, B. C. Sales, D. Mandrus, and S. W. Tozer, *J. Phys. Soc. Jpn.* **78**, 084719 (2009).
- ²³M. M. Altarawneh, K. Collar, C. H. Mielke, N. Ni, S. L. Bud'ko, and P. C. Canfield, *Phys. Rev. B* **78**, 220505 (2008).
- ²⁴R. T. Gordon, H. Kim, N. Salovich, R. W. Giannetta, R. M. Fernandes, V. G. Kogan, T. Prozorov, S. L. Bud'ko, P. C. Canfield, M. A. Tanatar, and R. Prozorov, *Phys. Rev. B* **82**, 054507 (2010).
- ²⁵L. Dorosinskii, M. Indenbom, V. Nikitenko, A. Polyanskii, R. Prozorov, and V. Vlasko-Vlasov, *Physica C* **206**, 360 (1993).
- ²⁶R. T. Gordon, H. Kim, M. A. Tanatar, R. Prozorov, and V. G. Kogan, *Phys. Rev. B* **81**, 180501 (2010).
- ²⁷V. G. Kogan, *Phys. Rev. B* **80**, 214532 (2009).
- ²⁸V. G. Kogan, R. Prozorov, S. L. Bud'ko, P. C. Canfield, J. R. Thompson, J. Karpinski, N. D. Zhigadlo, and P. Miranovic, *Phys. Rev. B* **74**, 184521 (2006).
- ²⁹Q. Huang, Y. Qiu, W. Bao, M. A. Green, J. W. Lynn, Y. C. Gasparovic, T. Wu, G. Wu, and X. H. Chen, *Phys. Rev. Lett.* **101**, 257003 (2008).